iScience

CellPress
OPEN ACCESS

Article

Multi-omics analysis reveals underlying host responses in pediatric respiratory syncytial virus pneumonia

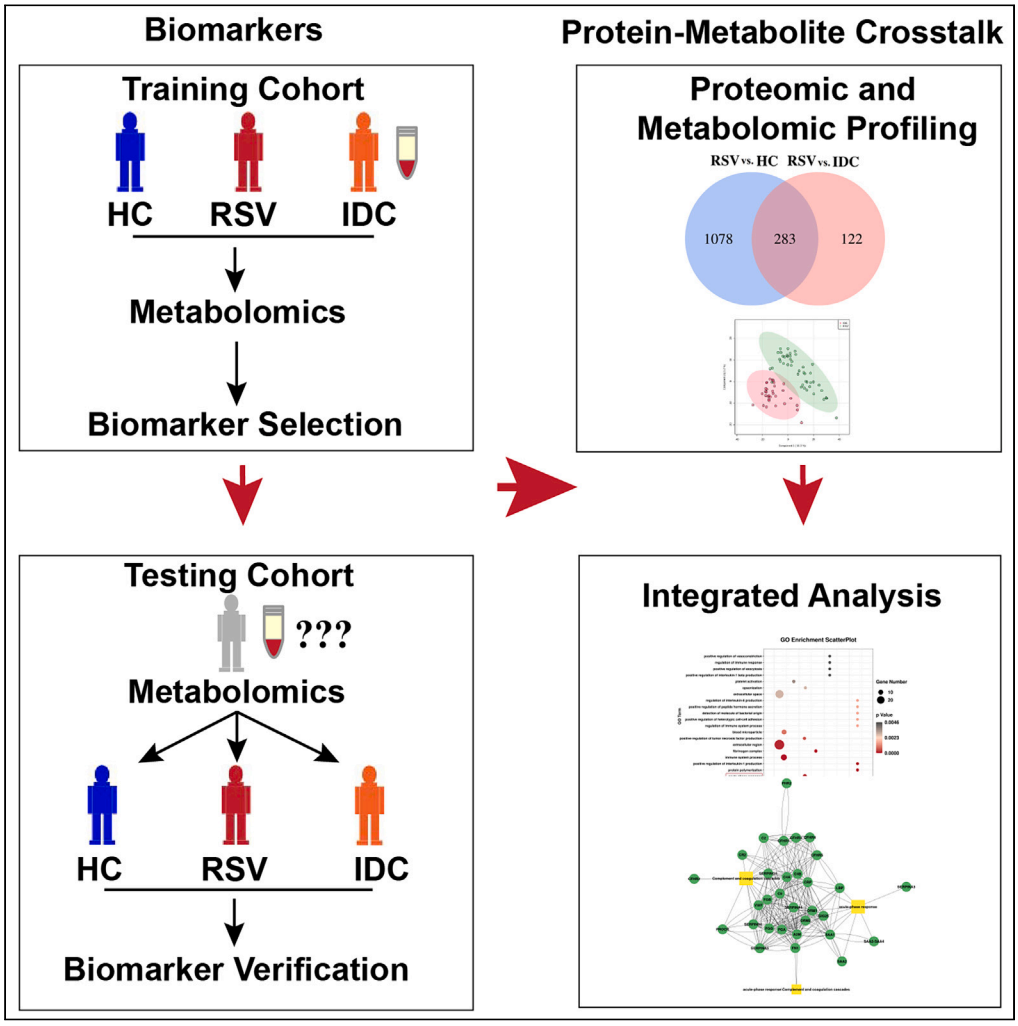

Xiaolan Huang, Fang Li, Yi Wang, ..., Laurence Don Wai Luu, Jun Tai, Jieqiong Li

wildwolf0101@163.com (Y.W.)
lizhenjun@icdc.cn (X.C.)
zjumedjun@163.com (D.Q.)
laurence.luu@uts.edu.au (L.D.W.L.)
trenttj@163.com (J.T.)
jieqiongli2010@163.com (J.L.)

Highlights

Two metabolic diagnostic markers were identified to distinguish RSV cases from controls

Integrated omics analysis revealed protein-metabolite crosstalk in RSV patients

Pathway analysis highlights increased collagen synthesis in RSV

Dysregulated lipid metabolism is a feature of RSV infection

Huang et al., iScience 26, 106329
April 21, 2023
https://doi.org/10.1016/j.isci.2023.106329

iScience

CellPress
OPEN ACCESS

Article

Multi-omics analysis reveals underlying host responses in pediatric respiratory syncytial virus pneumonia

Xiaolan Huang,[1,6] Fang Li,[2,6] Yi Wang,[1,6,*] Xinbei Jia,[3,6] Nan Jia,[1] Fei Xiao,[1] Chunrong Sun,[1] Jin Fu,[1] Min Chen,[1] Xiaodai Cui,[1,*] Dong Qu,[2,*] Laurence Don Wai Luu,[4,*] Jun Tai,[3,*] and Jieqiong Li[5,7,**]

SUMMARY

Respiratory syncytial virus (RSV) is an important pathogen causing pneumonia in children. Few studies have used multi-omics data to investigate the pathogenies of RSV pneumonia. Here, metabolomics was first used to identify potential biomarkers for RSV diagnosis. In the training cohort, serum from 36 healthy controls (HCs), 45 RSV pneumonia children, and 32 infectious disease controls (IDCs) were recruited. After analyses, six metabolites had potential diagnostic value. Using an independent cohort of 49 subjects, two biomarkers (neuromedin N and histidyl-proline diketopiperazine) were validated. Next, multi-omics analysis were applied to analyze the pathogenies of RSV pneumonia. Accumulation of collagen in the serum of RSVs indicated that RSV infection could lead to increased levels of soluble collage. Activation of the complement system and imbalance in lipid metabolism were also observed in RSV patients. The multi-omics analysis presented here revealed the signature protein and metabolite changes in serum caused by RSV infection.

INTRODUCTION

Pneumonia causes considerable global mortality among children, with an estimated 1.3 million deaths annually.[1,2] The primary pathogen in acute lower respiratory tract infection among children under five years old is respiratory syncytial virus (RSV), which affects 33.1 million children, resulting in 3.2 million hospitalizations and ~60,000 in-hospital deaths each year.[1,3] By the time children reach two years of age, most will have been infected with RSV. Although most show minor symptoms, 2–3% of children develop severe symptoms that require hospitalization and intensive care.

Despite efforts made to investigate the varying degree of host responses against RSV infection, the cause for why some children develop severe disease is still largely unknown. This suggests that there are multiple factors associated with RSV disease pathogenesis.[3] Previously, common pathological features in RSV infected patients were primarily studied using biopsy samples derived from critically ill cases. However, pathological and morphological characteristics are difficult to identify for mild RSV patients and thus the reason for differences in disease severity is unknown. Furthermore, efficient methods for diagnosing RSV infection are still limited.[4] Hence, knowledge about the molecular pathogenesis of RSV pneumonia is essential for guiding future diagnosis and treatment.

Recently, the advancement of multi-omic studies have aimed to identify diagnostic markers and shed light on the underlying molecular mechanism of different diseases.[5–7] Serum is a primary carrier of small molecules, whose relative concentrations can provide valuable insights into the pathogenesis of the disease. Previous RSV proteomic and metabolomic studies have revealed complicated cellular protein or metabolite landscapes and led to several findings related to RSV pathogenies.[8,9] For example, proteomics analyses indicated that RSV infection is associated with the glycolysis pathway and that this pathway may be targeted for the treatment of RSV infection.[10] Another proteomics study demonstrated that RSV replication led to global changes in the cellular proteome and remodeling of epigenetic regulatory complexes associated with the innate response.[11] A previous metabolomic analysis investigated the relationship between the metabolome of respiratory viruses infected patients with acute disease severity and asthma development.[12,13] However, most of these studies used single-omic data and to our knowledge,

[1]Experimental Research Center, Capital Institute of Pediatrics, Beijing 100020, P.R. China

[2]Department of Critical Medicine, Children's Hospital Affiliated Capital Institute of Pediatrics, Beijing 100020, P.R. China

[3]Department of Otolaryngology, Head and Neck Surgery, Children's Hospital Affiliated Capital Institute of Pediatrics, Beijing 100020, P. R. China

[4]School of Life Sciences, University of Technology Sydney, Sydney, NSW, Australia

[5]Medical Research Center, Beijing Institute of Respiratory Medicine and Beijing Chao-Yang Hospital, Capital Medical University, Beijing, China

[6]These authors contributed equally

[7]Lead contact

*Correspondence: wildwolf0101@163.com (Y.W.), lizhenjun@icdc.cn (X.C.), zjumedjun@163.com (D.Q.), laurence.luu@uts.edu.au (L.D.W.L.), trenttj@163.com (J.T.), jieqiongli2010@163.com (J.L.)

https://doi.org/10.1016/j.isci.2023.106329

there have been few studies that have used multi-omic data including both proteomics and metabolomics to investigate the pathogenies of RSV pneumonia.

Thus, to gain further insight into the molecular signatures of RSV pneumonia and for biomarker selection, we performed integrated metabolomic and proteomic analysis to study the protein and metabolite changes in the serum of RSV pneumonia patients (RSVs) compared to other infectious disease controls (IDCs) and healthy controls (HCs). The primary aim of this study was to identify metabolomic biomarkers for early and accurate diagnosis of RSV-infected children. The second aim was to determine the underlying molecular signatures in RSV-infected patients using protein-metabolite crosstalk analysis. Our RSV multi-omics analysis will help to provide early diagnostic methods and a better understanding of the pathogenesis of RSV pneumonia.

RESULTS

Research design and participants

To identify potential markers for RSV patients, we performed metabolomics profiling on serum samples from 162 subjects divided into two cohorts, a training cohort (cohort 1, n = 113, including 36 HCs, 45 RSVs, and 32 IDCs) and a testing cohort (cohort 2, n = 49, including 16 HCs, 19 RSVs, and 14 IDCs) (Figure 1A and Data S1). We used the metabolomic data from cohort 1 to identify characteristics of RSVs. Then, optimal biomarkers for diagnosis of RSV pneumonia were selected and further verified using metabolomics data from cohort 2 (Figure 1A). Characteristics and severity of patients were supplied in Data S1.

To characterize the protein-metabolite cross talk associated with RSV infection, 15 RSVs, 14 IDCs, and 15 HCs were randomly selected from each group for proteomic analysis. First, proteomic and metabolomic signatures were analyzed to provide a comprehensive molecular profile for RSVs. Next, the underlying mechanisms associated with RSV-induced host responses were assessed (Figure 1B). The clinical information and associated biochemical laboratory tests, collected from participants are shown in Data S2.

Selection of biomarkers for classification of RSV cases

To investigate the diagnostic value of DEMs, we first compared the metabolite differences between the RSV group and the HC or IDC group from cohort 1. PLS-DA models were used to compare the differences between RSVs with HCs (Figure 2A) and IDCs (Figure 2B). Clear differences were observed between the RSV and HC groups (cumulative R2 = 0.99338 and Q2 = 0.92319 [Figure 2C]), as well as between the RSV and IDC groups (cumulative R2 = 0.90954 and Q2 = 0.27064 [Figure 2D]). Compared to HCs and IDCs, there were 1361 and 405 DEMs (FC > 1.5 or FC < 0.67, $p < 0.05$) in the RSV group, respectively. Among them, 283 were overlapping (Figure 2E).

To evaluate their diagnostic value, we first calculated the AUC for these 283 overlapping DEMs, among which, six DEMs with an AUC > 0.8 were selected as potential biomarker candidates. Next, 5 machine learning classifiers, including logistic regression (Figure S1A), random forest (Figure S1B), linear support vector machine (Figure S1C), K-Nearest Neighbor (Figure S1D), and decision tree (Figure S1E) were used to determine the best diagnostic model while the 10-fold cross-validation method was used to evaluate their accuracy and error rate.

The AUC of the ROC curves calculated at optimal cutoffs for the six DEMs are shown in Figure 3A. The levels of neuromedin N, histidyl-proline diketopiperazine [Cyclo(His-Pro)], and estrone glucuronide were significantly increased in RSVs, while triacylglycerol (TG) (14:0/15:0/20:5(5Z,8Z,11Z,14Z,17Z)), pyridoxamine and 3-(1-Pyrazolyl)-alanine showed the opposite pattern (Figure 3B). Among them, neuromedin N showed the largest AUC of 0.948 and 0.842 when compared to HC and IDC, respectively. Additionally, the AUC for histidyl-proline diketopiperazine was 0.889 (Figure 3A) and 0.837 (Figure 3B) when compared to HC and IDC, respectively. The other 4 metabolites also showed high AUC-values, ranging from 0.801–0.953, when compared to HCs (Figure 3A) or IDCs (Figure 3B). In addition, we calculated the AUC-values for various combinations of these DEMs to differentiate RSV. As shown in Figure S1 and Data S3, the AUC of combined metabolites were not significantly higher than that of a single metabolite for discriminating RSV patients. Thus, considering simplicity and feasibility, we recommend that a single metabolite might be a more rational marker for RSV diagnosis.

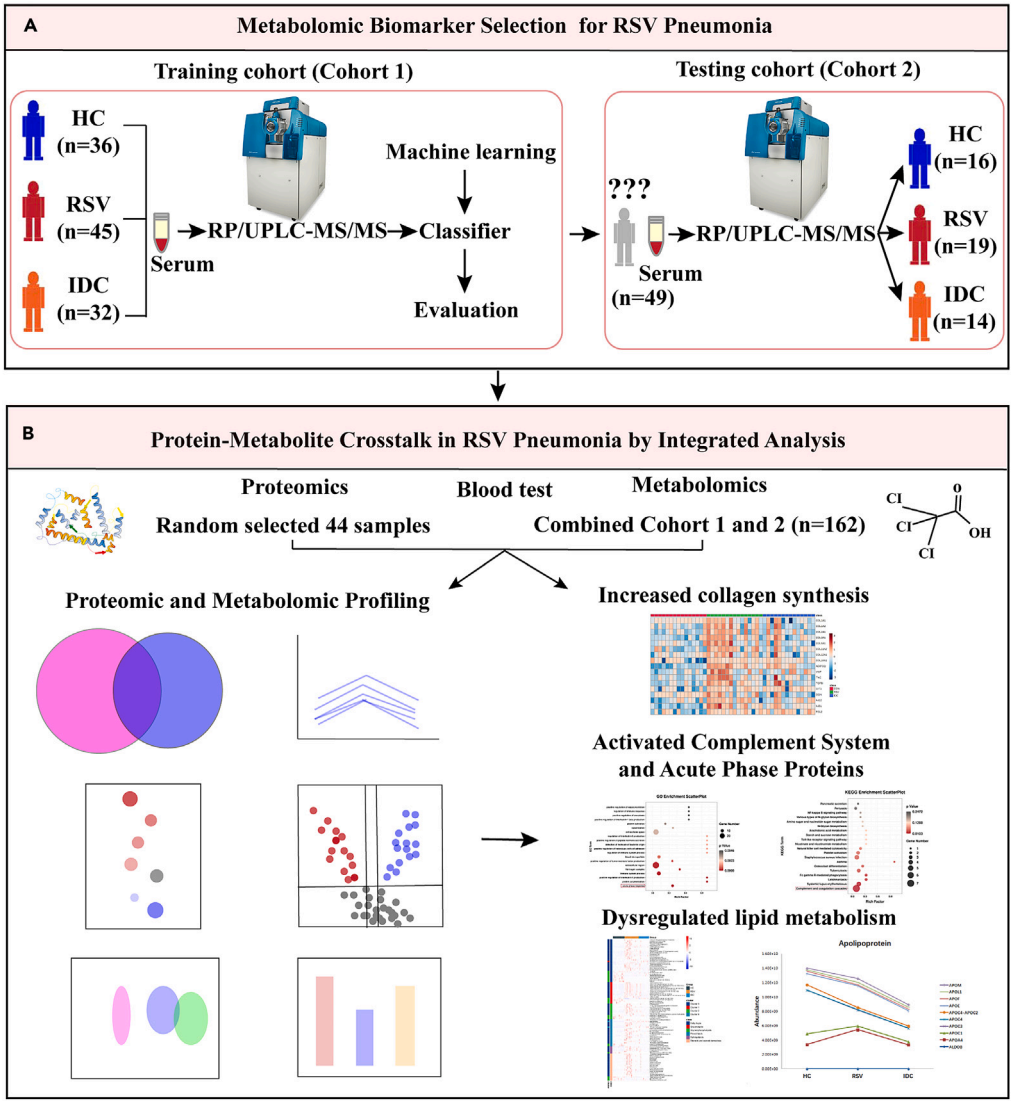

Figure 1. Study overview

(A) Study overview. 113 subjects including 36 HCs, 45 RSVs, and 32 IDCs from cohort 1 were recruited for metabolomic analysis. Data were analyzed to identify potential biomarkers for RSV diagnosis. Six biomarkers were further verified using an independent cohort with 49 blinded subjects.

(B) Protein-metabolite crosstalk was examined using integrated analysis. Proteomic and combined metabolomic signatures were analyzed for molecular profiles of RSV.

Independent validation of biomarkers

To validate our biomarkers, a randomized and blinded set based on metabolomics data from cohort 2 was used. As shown in Figure 3C, neuromedin N and histidyl-proline diketopiperazine had AUC values of 0.974 and 0.908 when RSV patients were compared to HCs, respectively. Additionally, neuromedin N (AUC, 0.816) and histidyl-proline diketopiperazine (AUC, 0.774) also showed relatively high AUCs when RSVs were compared to IDCs (Figure 3C). In contrast, the AUC for the other four metabolites (estrone glucuronide, TG (14:0/15:0/20:5[5Z,8Z,11Z,14Z,17Z]), pyridoxamine and 3-[1-Pyrazolyl]-alanine]) were lower than 0.7 as shown in Figure S2. Our results indicate the reliability of the two biomarkers (neuromedin N and histidyl-proline diketopiperazine) for distinguishing RSV from controls (Figure 3D).

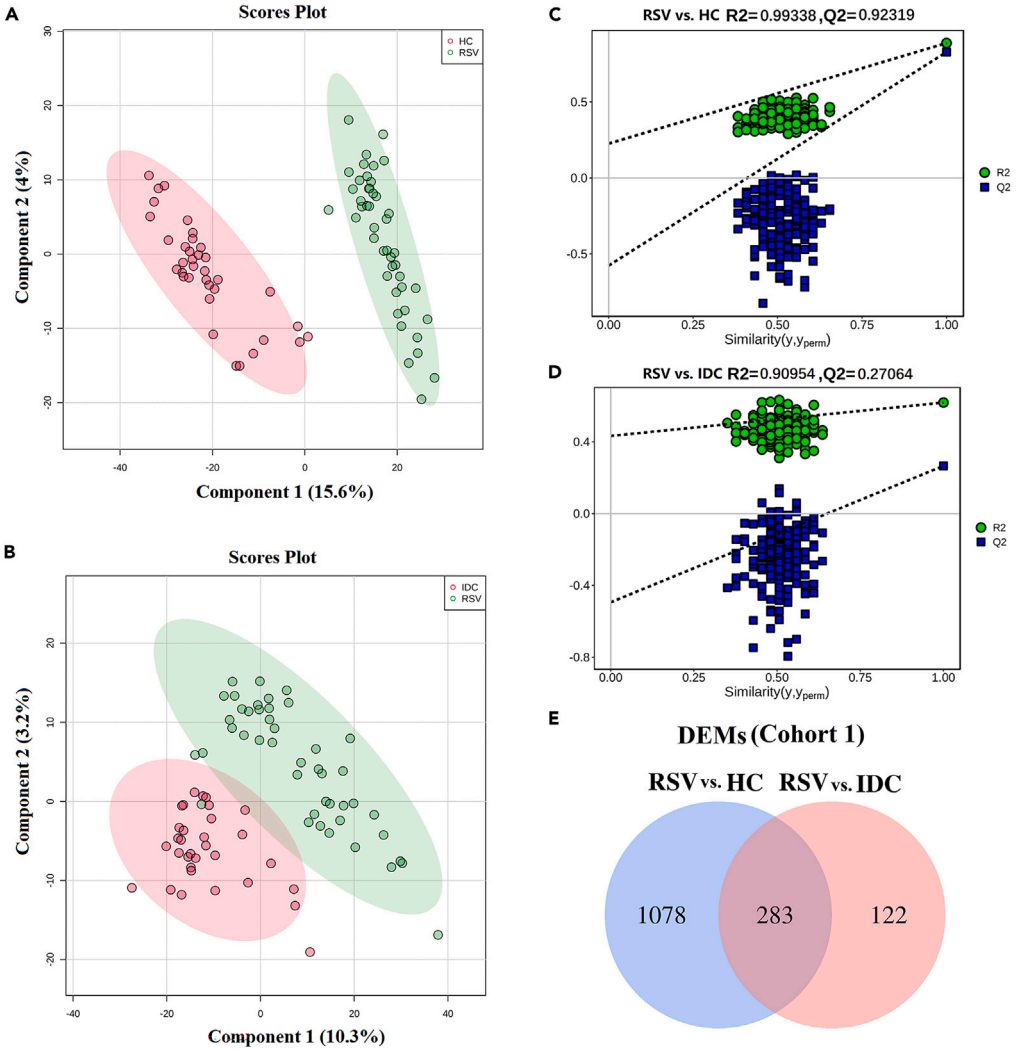

Figure 2. Identification of differentially expressed metabolites in RSVs from cohort 1

(A) PLS-DA score plots for RSVs and HCs.

(B) PLS-DA score plots for RSVs and IDCs.

(C) Parameters for assessing the quality of the PLS-DA model for RSVs and HCs.

(D) Parameters for assessing the quality of the PLS-DA model for RSVs and IDCs.

(E) DEMs identified in RSV children compared to IDCs and HCs.

Integrated protein-metabolite crosstalk analysis in RSV patients

Proteomic and metabolomic profiling of RSV pneumonia

To investigate the protein-metabolites cross talk in RSV pneumonia, 44 samples including 15 RSVs, 14 IDCs, and 15 HCs were randomly selected for proteomic analysis. After data preprocessing and protein identification, a total 211 DEPs were identified (Figure S3A and Data S4.1). PLS-DA illustrated evident differences in serum protein profiles (Figure S3B), and volcano plots from proteomic analyses show the number of DEPs (Figures S3C and S3D). KEGG enrichment analysis showed the main pathways associated with RSVs infection (Figures S3E and S3F). For the metabolomic analysis, the data from cohort 1 and cohort 2 were combined to investigate the metabolomic characteristics of RSVs. Compared to HCs and IDCs, a total of 1482 DEMs were identified in RSV patients (Figure S4A and Data S4.2). Similarly, PLS-DA (Figure S4B), volcano plots (Figures S4C and S4D), and KEGG analysis (Figures S4E and S4F) all illustrated evident differences in serum metabolite profiles.

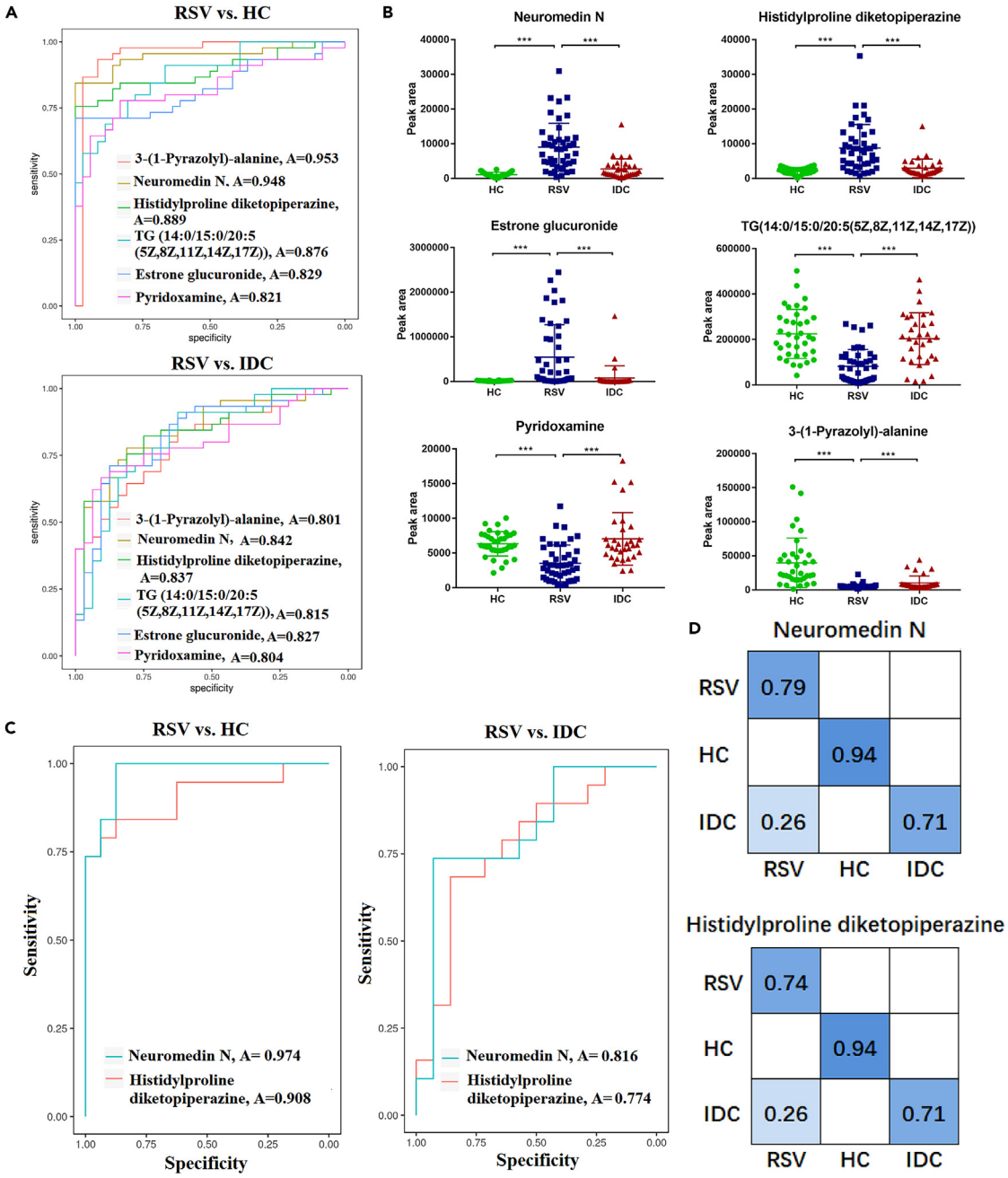

Figure 3. Identification and verification of potential biomarkers for classification of RSVs

(A) AUC values for six biomarkers were calculated to differentiate RSVs from HCs and IDCs in cohort 1.

(B) Expression levels of the sixpotential biomarkers across threegroups from cohort 1. The square and bars represent the mean and standard deviation, respectively. p values were calculated using Student's t test and significant p values are shown in the boxplot. ***p value < 0.001.

(C) AUC values for neuromedin N and histidyl-proline diketopiperazine [Cyclo(His-Pro)] were calculated to identify RSVs from HCs and IDCs in cohort 2.

(D) The confusion matrix for neuromedin N and histidyl-proline diketopiperazine [Cyclo(His-Pro)] among different serum samples from cohort 2.

Next, we observed that the 211 DEPs fell into four expression patterns, including two inverted "V" clusters (cluster 1 and cluster 3), an increasing cluster (cluster 2), and a decreasing cluster (cluster 4) (Figure 4A and Data S5.1). To characterize the dysregulated proteomic pathways in RSVs compared to controls, we performed pathway enrichment analyses for each cluster. Intriguingly, proteins in cluster 1 and 3 were primarily involved in focal adhesion and extracellular matrix-receptor interaction pathway (Figure 4B and Data S5.2).

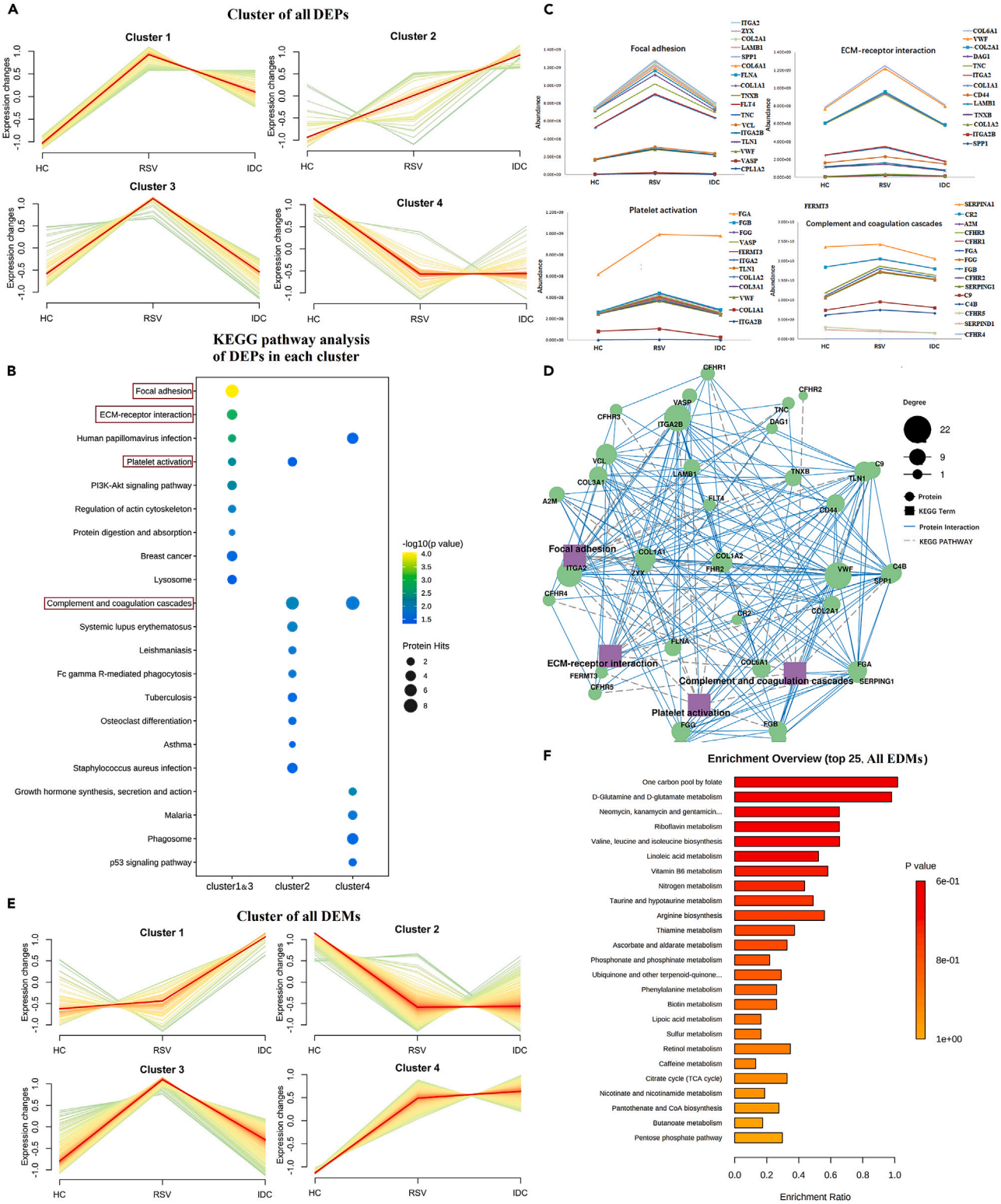

Figure 4. Differentially expressed proteins and metabolites in RSVs

(A) Hierarchical clustering shows four DEP patterns across 3 groups.

(B) KEGG terms enriched in clusters 1, and 3, cluster 2 and cluster 4. The top 10 KEGG terms are shown. Red lines highlight focal adhesion, ECM-receptor interaction, platelet activation, and complement and coagulation cascade pathways.

Figure 4. *Continued*

(C) Changes in proteins associated with focal adhesion, ECM-receptor interaction, platelet activation, and complement and coagulation cascades across three groups.

(D) The interaction diagram for proteins involved in the focal adhesion pathway, ECM-receptor interaction pathway, platelet activation pathway, and complement and coagulation cascade pathway. Purple squares represent pathways; green circles represent the altered proteins; dotted lines represent the association between the pathways and proteins. Solid lines represent associations between proteins.

(E) Hierarchical clustering shows four DEM patterns across three groups.

(F) KEGG analysis of all DEMs identified from RSVs compared to HCs and IDCs.

Here, we found that most proteins associated with focal adhesion and ECM-receptor interaction pathways were increased in RSVs compared to HCs and IDCs (Figure 4C and Data S5.2), supporting decreased wound repair function in RSV patients. For cluster 2 (increasing) and cluster 4 (decreasing), these proteins were primarily involved in the platelet activation pathway and the complement and coagulation cascade pathways (Figure 4B and Data S5.2). Moreover, these proteins combined to create a complex network, indicating the comprehensive diagram of DEPs (Figure 4D).

DEMs could also be classified into four expression patterns (Figure 4E and Data S5.3), and multiple metabolic pathways showed distinct profiles (Figure S5 and Data S5.4). Of note, KEGG analysis of all DEMs indicated that one carbon pool by folate, as well as D-glutamine and D-glutamate metabolism were the top essential pathways associated with RSV pneumonia (Figure 4F).

Increased collagen synthesis after RSV infection

Emerging evidence has demonstrated that RSV infection is a significant risk factor for pediatric asthma;[14] however, the underlying mechanism remains unclear. Collagen deposition results in an increase in matrix stiffness in asthma,[15,16] and we surprisingly found that DEPs from the inverted "V" clusters (cluster 1 and cluster 3) were involved in the collagen fibril organization pathway (Figure 5A). Accordingly, levels of collagen including type I (COL1A2), II (COL2A1), III (COL3A1), VI (COL6A1), XI (COL11A2), and XVIII (COL18A1) were elevated in RSVs compared to HCs (Figure 5B). In particular, levels of COL1A2, COL6A1, and COL11A2 in RSVs were also higher than that in IDCs (Figure 5C). Other extracellular matrix proteins such as nidogen (NID)1, NID2, and transforming growth factor (TGFBI) also showed similar trends (Figure 5B). Furthermore, the modules of proteins clustered into connected groups, reflecting their functional lineage relationship (Figure 5D). Collectively, since RSV infection may be associated with the occurrence of asthma, the increase in collagen levels is likely to be an important basis for predicting the occurrence of asthma after infection.

Activated complement system and acute phase proteins

As an important effector component of innate immunity, the complement system may cause damage to the host and can lead to inflammation.[17,18] As shown in Figure 6A, KEGG analysis of proteins in cluster 2 were primarily involved in complement and coagulation cascade pathways. The expression levels of fibrinogen alpha chain (FGA, FGB, and FGG) and complement related proteins (C2 and C4b) were increased in RSVs compared to HCs (Figure 6B). Interestingly, complement factor H related (CFHR) proteins, including CFHR1, CFHR2, CFHR3, CFHR4, and CFHR5 were all decreased in RSVs compared to HCs (Figure 6C). Moreover, levels of CFHR2, CFHR3, and CFHR5 were also lower in RSVs than that in IDCs (Figure 6C), suggesting that the effect on complement factor H was specific to RSV infections.

Additionally, GO-BP analysis also indicated that proteins in cluster 2 were mainly involved in acute-phase response pathways (Figure 6D). Here, we observed increased expression of acute-phase proteins such as CRP, lipopolysaccharide-binding protein (LBP) and serum amyloid A (SAA)1 in both RSV and IDC groups compared to the HC group. Other acute-phase proteins such as alpha-1-acid glycoprotein (ORM)1, ORM2, and SAA2 were only increased in IDCs compared to HCs and RSVs (Figure 6E). Moreover, proteins in the complement and acute-phase response pathways combined to create a complex network (Figure 6F). Collectively, the complement system, which plays a vital role in the eradication of pathogens, were also activated in RSV patients and contributed to the acute phase response.

Dysregulated lipid metabolism

Our data indicated changes to multiple apolipoproteins in RSVs including apolipoprotein A (APOA)4, APOC1, APOC3, APOC4, APOC4-APOC2, APOE, APOF, APOL1, and APOM (Figure 7A). When compared

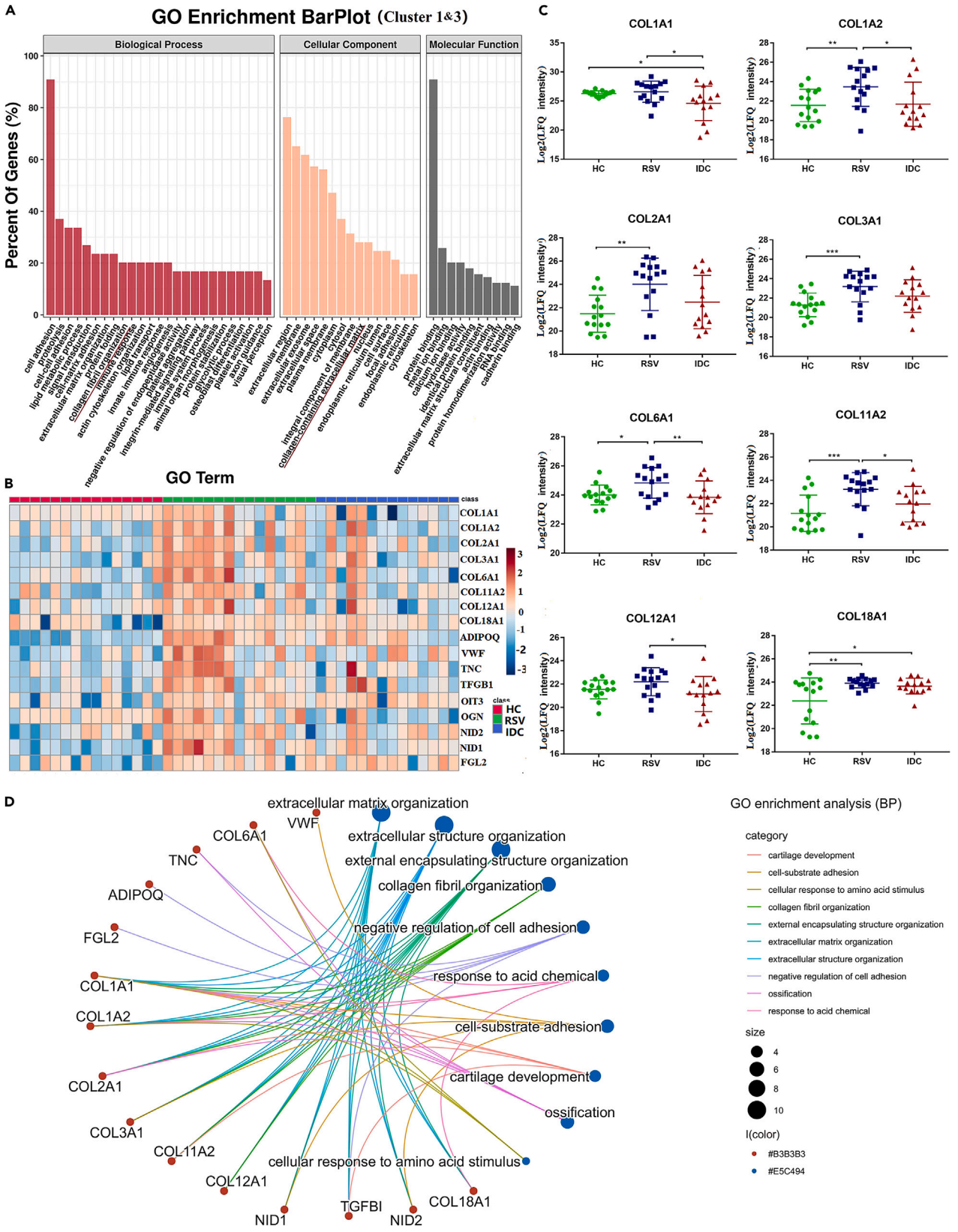
A
GO Enrichment BarPlot (Cluster 1&3)
Biological Process
Cellular Component
Molecular Function
Percent Of Genes (%)
B
GO Term
class
HC
RSV
IDC
C
COL1A1
COL1A2
COL2A1
COL3A1
COL6A1
COL11A2
COL12A1
COL18A1
Log2(LFQ intensity)
D
extracellular matrix organization
extracellular structure organization
external encapsulating structure organization
collagen fibril organization
negative regulation of cell adhesion
response to acid chemical
cell-substrate adhesion
cartilage development
ossification
cellular response to amino acid stimulus
GO enrichment analysis (BP)
category
cartilage development
cell-substrate adhesion
cellular response to amino acid stimulus
collagen fibril organization
external encapsulating structure organization
extracellular matrix organization
extracellular structure organization
negative regulation of cell adhesion
ossification
response to acid chemical
size
l(color)

Figure 5. Increased collagen synthesis in RSV infection

(A) GO enrichment analysis of the DEPs from clusters 1 and 3.

(B) Heatmap showing expression levels of proteins related to collagen fibril organization.

(C) Expression level of collagen proteins across three groups. Square and bars represent the mean and standard deviation, respectively. P values were calculated using Student's t test and significant p values are shown in the boxplot. *p value < 0.05, **p value < 0.01, and ***p value < 0.001.

(D) The interaction diagram of collagen proteins and pathways. Blue circles represent pathways; red circles represent the altered proteins; dotted lines represent the association between the pathways and proteins.

to HCs, some of these apolipoproteins were upregulated, while some were downregulated (Figure 7B). However, when compared to IDCs, most of these apolipoproteins were upregulated (Figure 7B). Consistent with our observations, the expression of APOL1 and APOM were also reduced in COVID-19 patients compared to controls.[19] Dysregulation of APOM has also been reported in the serum of HBV infected patients.[20] These results implied that lipid disorders occur in the pathogenesis of RSV infections.

Consistent with these proteomic findings, dysregulated lipid metabolism were also observed from our metabolomics data. Accumulation of 16 steroids and steroid derivatives, which may contribute to the modulation of macrophages, were observed in the serum of RSV patients (Figures 7C and 7D). Steroid hormones help boost the activity of macrophages and other immune cells.[21] Thus, the higher expression of steroids and steroid derivatives in RSVs suggests a protective function for steroid hormones against RSV infection.

Macrophage activity is closely related to lipid metabolism. Over 70 lipids were upregulated in RSV patients. Our data showed increased glycerolipids, glycerophospholipids, and sphingolipids in RSVs compared with both HCs and IDCs (Figure 7D). Sphingolipids and glycerophospholipids are essential components for signal transduction and immune activation. Sphingolipids regulate a variety of processes including migration, adhesion, apoptosis, and inflammation.[22] In conclusion, decreased lipids in RSV indicate activation of the immune response and damage of biomembranes after RSV infection.

DISCUSSION

RSV infection in children may cause life-threatening disease and is a serious threat to children's health.[1] There is an urgent need to identify novel biomarkers for early and accurate diagnosis, which will allow faster commencement of treatment interventions and improve disease outcomes. Here, we identified DEMs between RSVs and HCs or IDCs using metabolomics. After validation study, we confirmed the potential diagnostic value of two DEMs, neuromedin N, and histidyl-proline diketopiperazine, for RSV pneumonia. To our knowledge, this is the first study to show differential serum metabolic signatures during RSV pneumonia compared to both HCs and IDCs.

In a previous metabolomic correlation analysis, neuromedin N was reported to be a metabolite significantly associated with angiotensin-converting-enzyme inhibitors.[23] Here, we found that the expression of neuromedin N were significantly elevated in RSVs compared to both HCs and IDCs. In the training cohort, the AUC of neuromedin was 0.9481481 and 0.842361 when compared with HC and IDC, respectively. In the testing cohort, neuromedin N also showed a high AUC for RSV diagnosis. Cyclo (His-Pro) is an endogenous cyclic dipeptide and reported to be a potential anti-inflammatory molecule. Previous research indicates that cyclo (His-Pro) suppresses LPS-induced activation of NF-κB, and the NLRP3 inflammasome cascade; thus, leading to decreased cytokine production and decreased expression of induced nitrogen monoxide synthase (iNOS) and cyclooxygenase (COX2).[24,25] Thus, these effects suggest that cyclo (His-Pro) might be a potential anti-inflammatory molecule. In this study, we observed that the expression of cyclo (His-Pro) was significantly elevated in RSVs compared to controls, suggesting that the anti-inflammatory effects were accompanied by RSV infection. Our results indicate that cyclo (His-Pro) is also a potential diagnostic marker for RSV pneumonia in children.

Extracellular matrix deposition is a feature of airway remodeling after prolonged allergen challenge. It has been reported that RSV infection attenuates epithelial migration and leads to slower wound healing.[26] In this study, we found that proteins in the inverted "V" clusters (cluster 1 and cluster 3) were primarily involved in the collagen fibril organization pathway. In RSVs, the levels of most collagen, such as COL1A2, COL1A1, COL2A1, COL3A1, COL6A1, COL11A2, and COL12A1 were significantly higher than controls. These results suggest that RSV infection may lead to increased levels of soluble collagen, which

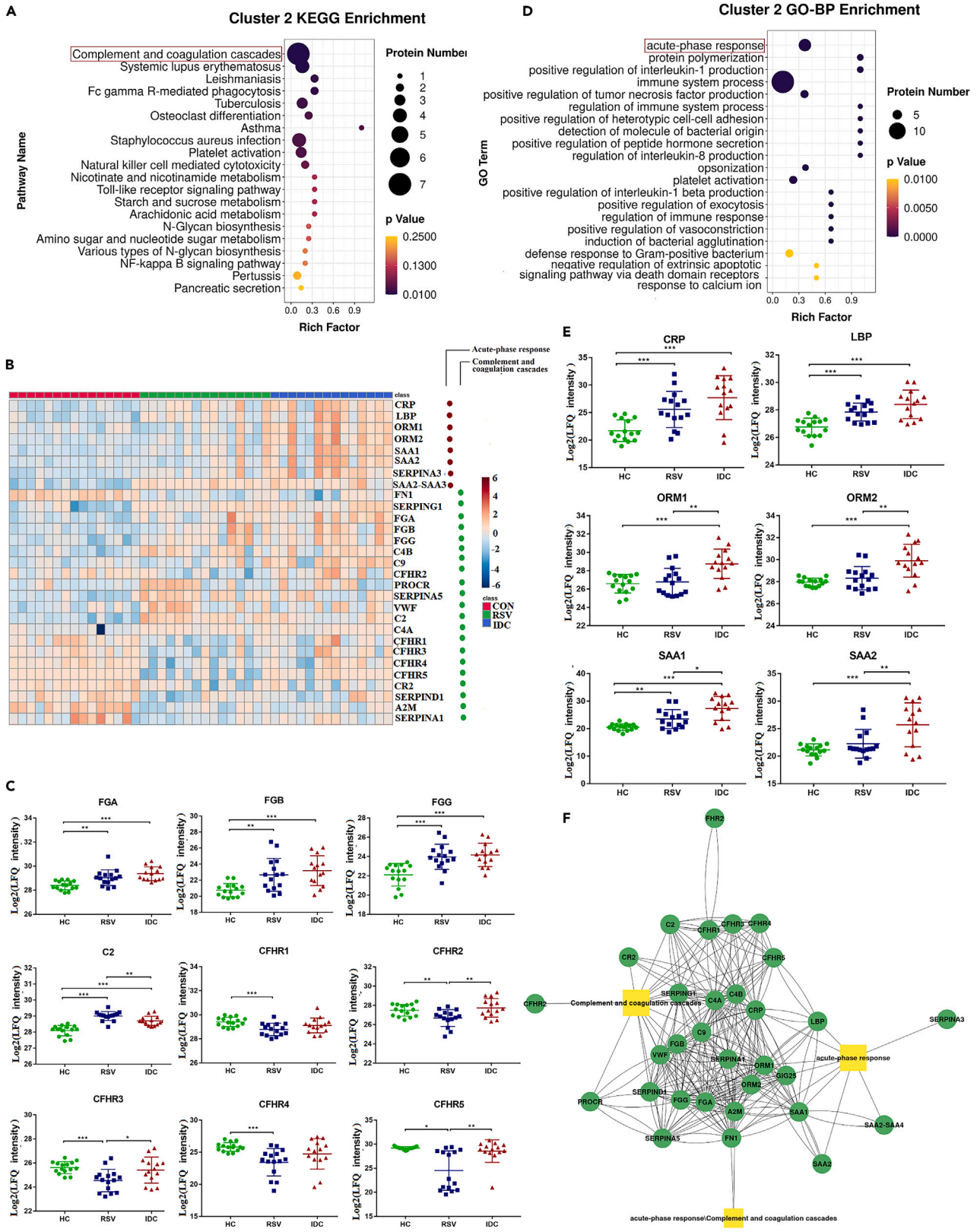
A
Cluster 2 KEGG Enrichment
Complement and coagulation cascades
Systemic lupus erythematosus
Leishmaniasis
Fc gamma R-mediated phagocytosis
Tuberculosis
Osteoclast differentiation
Asthma
Staphylococcus aureus infection
Platelet activation
Natural killer cell mediated cytotoxicity
Nicotinate and nicotinamide metabolism
Toll-like receptor signaling pathway
Starch and sucrose metabolism
Arachidonic acid metabolism
N-Glycan biosynthesis
Amino sugar and nucleotide sugar metabolism
Various types of N-glycan biosynthesis
NF-kappa B signaling pathway
Pertussis
Pancreatic secretion
Pathway Name
Rich Factor
Protein Numbe
p Value
D
Cluster 2 GO-BP Enrichment
acute-phase response
protein polymerization
positive regulation of interleukin-1 production
immune system process
positive regulation of tumor necrosis factor production
regulation of immune system process
positive regulation of heterotypic cell-cell adhesion
detection of molecule of bacterial origin
positive regulation of peptide hormone secretion
regulation of interleukin-8 production
opsonization
platelet activation
positive regulation of interleukin-1 beta production
positive regulation of exocytosis
regulation of immune response
positive regulation of vasoconstriction
induction of bacterial agglutination
defense response to Gram-positive bacterium
negative regulation of extrinsic apoptotic signaling pathway via death domain receptors
response to calcium ion
GO Term
Rich Factor
Protein Number
p Value
B
Acute-phase response
Complement and coagulation cascades
class
CRP
LBP
ORM1
ORM2
SAA1
SAA2
SERPINA3
SAA2-SAA3
FN1
SERPING1
FGA
FGB
FGG
C4B
C9
CFHR2
PROCR
SERPINA5
VWF
C2
C4A
CFHR1
CFHR3
CFHR4
CFHR5
CR2
SERPIND1
A2M
SERPINA1
CON
RSV
IDC
E
CRP
LBP
ORM1
ORM2
SAA1
SAA2
Log2(LFQ intensity)
HC
RSV
IDC
C
FGA
FGB
FGG
C2
CFHR1
CFHR2
CFHR3
CFHR4
CFHR5
F
CFHR2
C2
CFHR1
CFHR3
CFHR4
CR2
CFHR5
SERPING1
C4A
C4B
CRP
LBP
SERPINA3
Complement and coagulation cascades
C9
FGB
VWF
SERPINA1
ORM1
SIG23
acute-phase response
ORM2
SERPIND1
FGG
FGA
A2M
SAA1
SAA2-SAA4
PROCR
SERPINA5
FN1
SAA2
acute-phase response\Complement and coagulation cascades

Figure 6. Activated complement system and acute phase proteins

(A) KEGG enrichment analysis of DEPs from cluster 2. The top 20 GO-BP terms are shown.

(B) Heatmap depicting expression levels of proteins associated with the complement and coagulation cascade pathways and acute-phase response pathways in HCs, RSVs, and IDCs.

(C) Expression level of proteins associated with the complement and coagulation cascade pathways.

(D) GO-BP enrichment analysis of the DEPs from cluster 2. The top 20 GO-BP terms are shown.

(E) Expression level of proteins associated with the acute-phase response pathway. The square and bars represent the mean and standard deviation, respectively. p values were calculated using Student's t test and significant p values are shown in the boxplot. *p value < 0.05, **p value < 0.01, and ***p value < 0.001.

(F) The interaction diagram of proteins and pathways. Yellow squares represent pathways; green circles represent altered proteins; dotted lines represent the association between the pathways and proteins.

helps stimulate airway remodeling of the lung. Previous studies have found that RSV infection of ovalbumin-sensitized mice results in chronic airway inflammation, along with increased collagen deposition.[27,28] Here, the deposition of collagens was also observed in the serum samples of RSV infected children, consistent with previous studies. KEGG analysis of all DEMs indicated that one carbon pool by folate, as well as D-glutamine and D-glutamate metabolism were essential to RSV pneumonia. One-carbon metabolism is driven by the folate and methionine cycles, which together regulate the synthesis of DNA. Moreover, dysregulated one-carbon metabolism intermediates can induce aberrant immune responses, which may be involved in RSV infection.[29]

It has been reported that activation of the complement system could help to suppress viral invasion.[30] In this study, our data showed fibrinogen alpha chain (FGA, FGB, and FGG) and complement related proteins (C2 and C4b) were increased in RSVs compared to HCs, which suggests activation of the complement system after RSV infection. On the contrary, complement factor H related proteins, including CFHR1, CFHR2, CFHR3, CFHR4, and CFHR5, were significantly decreased in RSVs compared to controls. FGA, FGB, and FGG are the main components of fibrinogen. Fibrinogen and other components have been reported to influence the inflammatory process through a variety of pathways.[31] Complement factor H is the major negative regulators of complement activation, whose variation is associated with susceptibility to both rare and common diseases. Downregulation of complement factor H reduces its negative regulatory effect, which leads to the overactivation of the complement system.[32] Thus, dysregulation of the complement system may be involved in the pathogenesis of RSV, and targeting the CFHR protein family might be an effective way to restore complement regulation. It was shown that CFHR1, CFHR4, and CFHR5 can act as a platform for assembling C3bBbP convertases and enhance activation of the alternative pathway.[32] Moreover, proteins in the complement and acute-phase response pathways combined to create a complex network. Levels of CRP, LBP, and SAA 1 were increased in IDCs were increased in both RSV and IDC groups compared to the HC group. Expression of ORM1, ORM2, and SAA2 were increased in IDCs. ORM1, ORM2, SAA1, SAA2, and CRP in serum have been reported to be associated with inflammation and infection.[19] Among these proteins, the expression of SAA1 was also differentially expressed between RSVs and IDCs. SAA1 has been previously reported to be an important marker for viral infection.[33] Collectively, our results suggest excessive activation of the complement system and inflammation in RSVs and this activation may lead to severe damage.

Our metabolomics results showed that various types of lipids such as glycerophospholipid, sphingolipid, and fatty acids were significantly decreased in RSVs, which may reflect aberrancy in bilirubin and bile acids. Glycerophospholipids and sphingolipids are involved in the early development of enveloped viruses.[34] RSV infection leads to specific changes in lipids, which play a key role in virus maturation.[35] Lipid metabolism is also involved in the pathogenesis of RSV. It was reported that RSV can promote lipid dispersion and utilization, resulting in expanded oxidative damage and a surge in proinflammatory cytokines, leading to the development of airway hyperresponsiveness.[36] Additionally, drugs used to inhibit lipid synthesis have been proposed to treat viral infections.[37,38] Our results suggest that these potential therapeutics targeting lipid metabolism regulation might be useful for RSV treatment.

The highlight of this study was the use of disease controls in children with RSV infection. Our study selected and verified diagnostic metabolomic biomarkers and revealed the proteomic and metabolic characteristics of RSV-infected children. Because serum samples collected from RSVs, IDCs, and HCs were age and sex-matched, the variation in protein and metabolite concentrations due to these two factors was minimized.

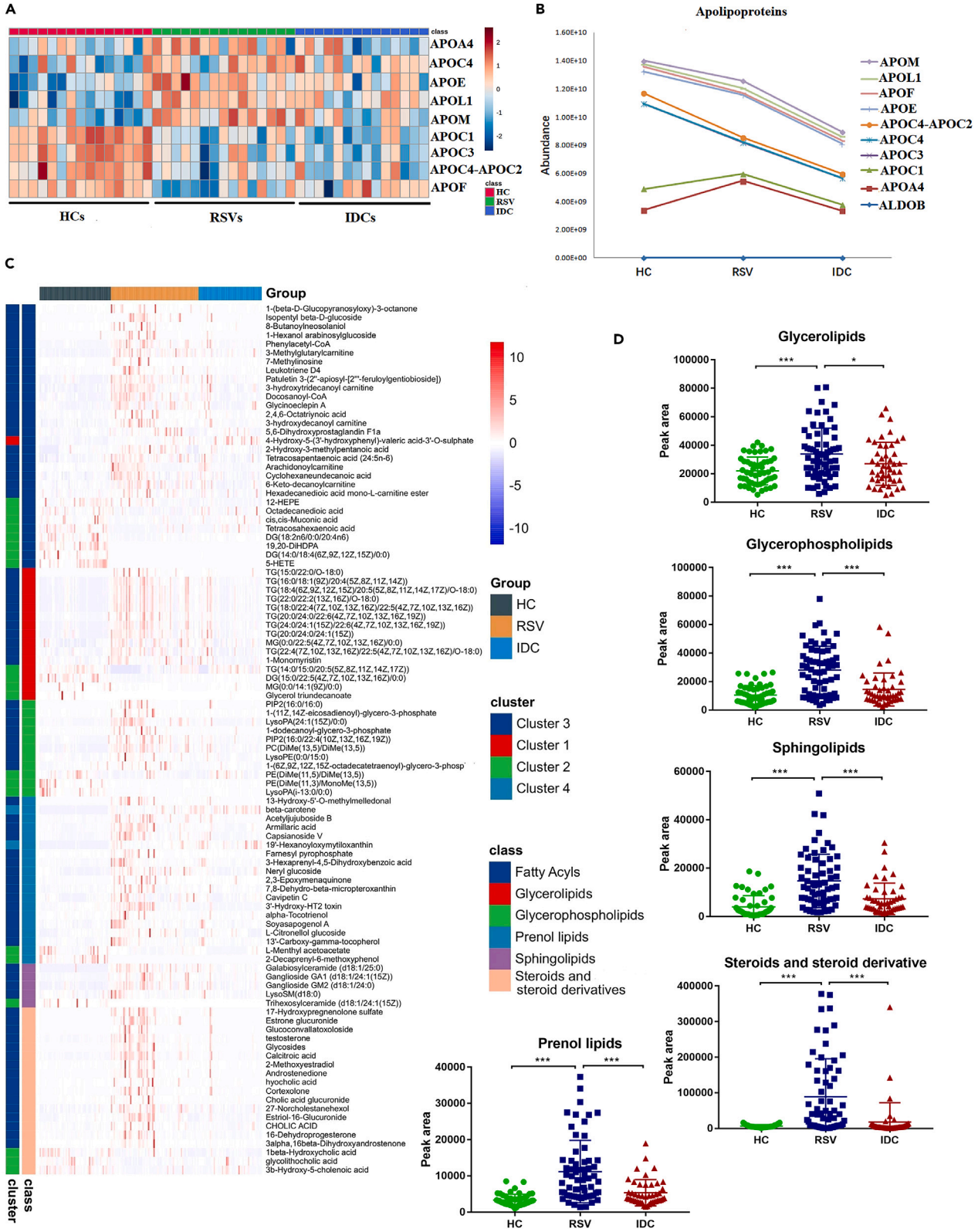
A
class
APOA4
APOC4
APOE
APOL1
APOM
APOC1
APOC3
APOC4-APOC2
APOF
HCs
RSVs
IDCs
class
HC
RSV
IDC
B
Apolipoproteins
Abundance
APOM
APOL1
APOF
APOE
APOC4-APOC2
APOC4
APOC3
APOC1
APOA4
ALDOB
HC
RSV
IDC
C
Group
cluster
class
HC
RSV
IDC
Cluster 3
Cluster 1
Cluster 2
Cluster 4
Fatty Acyls
Glycerolipids
Glycerophospholipids
Prenol lipids
Sphingolipids
Steroids and steroid derivatives
D
Glycerolipids
Glycerophospholipids
Sphingolipids
Steroids and steroid derivative
Prenol lipids
Peak area
***
*

Figure 7. Dysregulated lipid metabolism in RSV

(A) Heatmap showing expression levels of apolipoproteins in HCs, RSVs, and IDCs.

(B) Abundance levels of apolipoproteins across three groups.

(C) Heatmap of DEMs that are associated with fatty acyls, glycerolipids, glycerophospholipids, prenol lipids, sphingolipids, steroid, and steroid derivatives.

(D) Representative lipid expression changes across three groups. The square and bars represent the mean and standard deviation, respectively. p values were calculated using Student's t test and significant p values are shown in the boxplot. *p value < 0.05, and ***p value < 0.001.

In conclusion, a systematic proteomic and metabolomic study was performed on serum samples from RSV patients and controls. We demonstrated the potential to identify RSV patients using serum metabolites. Our study also provides a landscape view of the serum molecular changes induced by RSV infection, which may provide useful diagnostic and therapeutic information for RSV infections in children.

Limitations of the study

Although our samples were matched, there may be other genetic and environmental confounding factors that may not have been detected or controlled for. Furthermore, although our results were verified using an independent cohort, further verification using larger sample sizes is still required.

STAR★METHODS

Detailed methods are provided in the online version of this paper and include the following:

- KEY RESOURCES TABLE
- RESOURCE AVAILABILITY
  - Lead contact
  - Materials availability
  - Data and code availability
- EXPERIMENTAL MODEL AND SUBJECT DETAILS
  - Patient enrollment
  - Clinical information
- METHOD DETAILS
  - Metabolomic analysis
  - Proteomic analysis
- QUANTIFICATION AND STATISTICAL ANALYSIS
  - Statistical analysis of clinical data
  - Statistical analysis of multi-omics data

SUPPLEMENTAL INFORMATION

Supplemental information can be found online at https://doi.org/10.1016/j.isci.2023.106329.

ACKNOWLEDGMENTS

This work was supported by grants from the National Key Research and Development Program of China (Grant Nos. 2021YFC2301101, 2021YFC2301102), the public service development and reform pilot project of Beijing Medical Research Institute (BMR2019-11), and Beijing Social Science Foundation Project (19GLB033). Laurence Don Wai Luu was supported by a UTS Chancellor's Postdoctoral Research Fellowship. We thank all the participants. We gratefully acknowledge the participation of Fan-Xing Biological Technology Co., Ltd. (Tianjin) for the support of bioinformatics analysis with their analysis platform, and thank Miss Yan Li for her contribution. This study was approved by the Ethics Committee of the Capital Institute of Pediatrics (Ethical approval number: SHERLLM2019001). The lead author and guarantor affirm that the manuscript is an honest, accurate, and transparent account of the study being reported; that no important aspects of the study have been omitted; and that any discrepancies from the study as planned and registered have been explained.

AUTHOR CONTRIBUTIONS

Y.W. conceived the study. Y.W. and J.L. designed the study. Y.W., J.L., X.C., D.Q., J.T., supervised and controlled this project. F.L., X.H., X.J., N.J., F.X., C.S., J.F., and M.C. performed the experiments. Y.W., X.C., D.Q., and J.T. contributed the reagents and materials. J.L., Y.W., and L.D.W.L. contributed the analysis tools. J.L. and Y.W. performed the software. J.L., Y.W., and L.D.W.L. analyzed the data. J.L. and Y.W.

drafted the original paper. Y.W. and L.D.W.L. revised and edited this paper. Y.W., J.L., L.D.W.L., and J.T. reviewed the paper.

DECLARATION OF INTERESTS

The authors declare no competing interests.

INCLUSION AND DIVERSITY

We support inclusive, diverse, and equitable conduct of research.

Received: October 17, 2022
Revised: December 17, 2022
Accepted: February 28, 2023
Published: March 3, 2023

REFERENCES

1. Shi, T., McAllister, D.A., O'Brien, K.L., Simoes, E.A.F., Madhi, S.A., Gessner, B.D., Polack, F.P., Balsells, E., Acacio, S., Aguayo, C., et al. (2017). Global, regional, and national disease burden estimates of acute lower respiratory infections due to respiratory syncytial virus in young children in 2015: a systematic review and modelling study. Lancet *390*, 946–958. https://doi.org/10.1016/s0140-6736(17)30938-8.

2. Agweyu, A., Kibore, M., Digolo, L., Kosgei, C., Maina, V., Mugane, S., Muma, S., Wachira, J., Waiyego, M., and Maleche-Obimbo, E. (2014). Prevalence and correlates of treatment failure among Kenyan children hospitalised with severe community-acquired pneumonia: a prospective study of the clinical effectiveness of WHO pneumonia case management guidelines. Trop. Med. Int. Health *19*, 1310–1320. https://doi.org/10.1111/tmi.12368.

3. Tahamtan, A., Samadizadeh, S., Rastegar, M., Nakstad, B., and Salimi, V. (2020). Respiratory syncytial virus infection: why does disease severity vary among individuals? Expert Rev. Respir. Med. *14*, 415–423. https://doi.org/10.1080/17476348.2020.1724095.

4. Lee, N., Walsh, E.E., Sander, I., Stolper, R., Zakar, J., Wyffels, V., Myers, D., and Fleischhackl, R. (2019). Delayed diagnosis of respiratory syncytial virus infections in hospitalized adults: individual patient data, record review analysis and physician survey in the United States. J. Infect. Dis. *220*, 969–979. https://doi.org/10.1093/infdis/jiz236.

5. Li, J., Luu, L.D.W., Wang, X., Cui, X., Huang, X., Fu, J., Zhu, X., Li, Z., Wang, Y., and Tai, J. (2022). Metabolomic analysis reveals potential biomarkers and the underlying pathogenesis involved in Mycoplasma pneumoniae pneumonia. Emerg. Microbes Infect. *11*, 593–605. https://doi.org/10.1080/22221751.2022.2036582.

6. Wang, Y., Wang, X., Luu, L.D.W., Chen, S., Jin, F., Wang, S., Huang, X., Wang, L., Zhou, X., Chen, X., et al. (2022). Proteomic and metabolomic signatures associated with the immune response in healthy individuals immunized with an inactivated SARS-CoV-2 vaccine. Front. Immunol. *13*, 848961. https://doi.org/10.3389/fimmu.2022.848961.

7. Huang, X., Luu, L.D.W., Jia, N., Zhu, J., Fu, J., Xiao, F., Liu, C., Li, S., Shu, G., Hou, J., et al. (2022). Multi-platform omics analysis reveals molecular signatures for pathogenesis and activity of systemic lupus erythematosus. Front. Immunol. *13*, 833699. https://doi.org/10.3389/fimmu.2022.833699.

8. Zhang, X., Peng, D., Zhang, X., Wang, X., Chen, N., Zhao, S., and He, Q. (2021). Serum metabolomic profiling reveals important difference between infants with and without subsequent recurrent wheezing in later childhood after RSV bronchiolitis. APMIS *129*, 128–137. https://doi.org/10.1111/apm.13095.

9. Dapat, C., and Oshitani, H. (2016). Novel insights into human respiratory syncytial virus-host factor interactions through integrated proteomics and transcriptomics analysis. Expert Rev. Anti Infect. Ther. *14*, 285–297. https://doi.org/10.1586/14787210.2016.1141676.

10. Yin, G.Q., Zeng, H.X., Li, Z.L., Chen, C., Zhong, J.Y., Xiao, M.S., Zeng, Q., Jiang, W.H., Wu, P.Q., Zeng, J.M., et al. (2021). Differential proteomic analysis of children infected with respiratory syncytial virus. Braz. J. Med. Biol. Res. *54*, e9850. https://doi.org/10.1590/1414-431x20209850.

11. Mann, M., and Brasier, A.R. (2021). Evolution of proteomics technologies for understanding respiratory syncytial virus pathogenesis. Expert Rev. Proteomics *18*, 379–394. https://doi.org/10.1080/14789450.2021.1931130.

12. Fujiogi, M., Camargo, C.A., Jr., Raita, Y., Bochkov, Y.A., Gern, J.E., Mansbach, J.M., Piedra, P.A., and Hasegawa, K. (2020). Respiratory viruses are associated with serum metabolome among infants hospitalized for bronchiolitis: a multicenter study. Pediatr. Allergy Immunol. *31*, 755–766. https://doi.org/10.1111/pai.13296.

13. Fujiogi, M., Camargo, C.A., Jr., Raita, Y., Zhu, Z., Celedón, J.C., Mansbach, J.M., Spergel, J.M., and Hasegawa, K. (2021). Integrated associations of nasopharyngeal and serum metabolome with bronchiolitis severity and asthma: a multicenter prospective cohort study. Pediatr. Allergy Immunol. *32*, 905–916. https://doi.org/10.1111/pai.13466.

14. Jartti, T., Bønnelykke, K., Elenius, V., and Feleszko, W. (2020). Role of viruses in asthma. Semin. Immunopathol. *42*, 61–74. https://doi.org/10.1007/s00281-020-00781-5.

15. Liu, L., Stephens, B., Bergman, M., May, A., and Chiang, T. (2021). Role of collagen in airway mechanics. Bioengineering *8*, 13. https://doi.org/10.3390/bioengineering8010013.

16. Hocking, D.C. (2002). Fibronectin matrix deposition and cell contractility: implications for airway remodeling in asthma. Chest *122*, 275s–278s. https://doi.org/10.1378/chest.122.6_suppl.275s.

17. Garred, P., Tenner, A.J., and Mollnes, T.E. (2021). Therapeutic targeting of the complement system: from rare diseases to pandemics. Pharmacol. Rev. *73*, 792–827. https://doi.org/10.1124/pharmrev.120.000072.

18. Hajishengallis, G., Reis, E.S., Mastellos, D.C., Ricklin, D., and Lambris, J.D. (2017). Novel mechanisms and functions of complement. Nat. Immunol. *18*, 1288–1298. https://doi.org/10.1038/ni.3858.

19. Shen, B., Yi, X., Sun, Y., Bi, X., Du, J., Zhang, C., Quan, S., Zhang, F., Sun, R., Qian, L., et al. (2020). Proteomic and metabolomic characterization of COVID-19 patient sera. Cell *182*, 59–72.e15. https://doi.org/10.1016/j.cell.2020.05.032.

20. Gu, J.G., Zhu, C.L., Cheng, D.Z., Xie, Y., Liu, F., and Zhou, X. (2011). Enchanced levels of apolipoprotein M during HBV infection feedback suppresses HBV replication. Lipids Health Dis. *10*, 154. https://doi.org/10.1186/1476-511x-10-154.

21. Cain, D.W., and Cidlowski, J.A. (2017). Immune regulation by glucocorticoids. Nat. Rev. Immunol. *17*, 233–247. https://doi.org/10.1038/nri.2017.1.

22. Hannun, Y.A., and Obeid, L.M. (2018). Sphingolipids and their metabolism in physiology and disease. Nat. Rev. Mol. Cell Biol. *19*, 175–191. https://doi.org/10.1038/nrm.2017.107.

23. Liang, Y.J., Lin, Y.T., Chen, C.W., Lin, C.W., Chao, K.M., Pan, W.H., and Yang, H.C. (2016). SMART: statistical metabolomics analysis-an R tool. Anal. Chem. *88*, 6334–6341. https://doi.org/10.1021/acs.analchem.6b00603.

24. Grottelli, S., Mezzasoma, L., Scarpelli, P., Cacciatore, I., Cellini, B., and Bellezza, I. (2019). Cyclo(His-Pro) inhibits NLRP3 inflammasome cascade in ALS microglial cells. Mol. Cell. Neurosci. *94*, 23–31. https://doi.org/10.1016/j.mcn.2018.11.002.

25. Grottelli, S., Ferrari, I., Pietrini, G., Peirce, M.J., Minelli, A., and Bellezza, I. (2016). The role of cyclo(His-Pro) in neurodegeneration. Int. J. Mol. Sci. *17*, 1332. https://doi.org/10.3390/ijms17081332.

26. Linfield, D.T., Gao, N., Raduka, A., Harford, T.J., Piedimonte, G., and Rezaee, F. (2021). RSV attenuates epithelial cell restitution by inhibiting actin cytoskeleton-dependent cell migration. Am. J. Physiol. Lung Cell Mol. Physiol. *321*, L189–L203. https://doi.org/10.1152/ajplung.00118.2021.

27. Wang, J.H., Sun, L.H., Huang, S.K., and Chen, A.H. (2016). Effect of co-culturing human primary basic fibroblasts with respiratory syncytial virus-infected 16-HBE cells. Genet. Mol. Res. *15*. https://doi.org/10.4238/gmr.15017339.

28. Tourdot, S., Mathie, S., Hussell, T., Edwards, L., Wang, H., Openshaw, P.J.M., Schwarze, J., and Lloyd, C.M. (2008). Respiratory syncytial virus infection provokes airway remodelling in allergen-exposed mice in absence of prior allergen sensitization. Clin. Exp. Allergy *38*, 1016–1024. https://doi.org/10.1111/j.1365-2222.2008.02974.x.

29. Lyon, P., Strippoli, V., Fang, B., and Cimmino, L. (2020). B vitamins and one-carbon metabolism: implications in human health and disease. Nutrients *12*, 2867. https://doi.org/10.3390/nu12092867.

30. Barnum, S.R. (2017). Complement: a primer for the coming therapeutic revolution. Pharmacol. Ther. *172*, 63–72. https://doi.org/10.1016/j.pharmthera.2016.11.014.

31. Hoppe, B. (2014). Fibrinogen and factor XIII at the intersection of coagulation, fibrinolysis and inflammation. Thromb. Haemost. *112*, 649–658. https://doi.org/10.1160/th14-01-0085.

32. Parente, R., Clark, S.J., Inforzato, A., and Day, A.J. (2017). Complement factor H in host defense and immune evasion. Cell. Mol. Life Sci. *74*, 1605–1624. https://doi.org/10.1007/s00018-016-2418-4.

33. Niu, T., Liu, Y., Zhu, F., Ma, J., and Gao, J. (2019). Time-resolved fluorescent immunoassay-based combined detection of procalcitonin, C-reactive protein, heparin binding protein, and serum amyloid A1 to improve the diagnostic accuracy of early infection. J. Clin. Lab. Anal. *33*, e22694. https://doi.org/10.1002/jcla.22694.

34. Schoggins, J.W., and Randall, G. (2013). Lipids in innate antiviral defense. Cell Host Microbe *14*, 379–385. https://doi.org/10.1016/j.chom.2013.09.010.

35. Yeo, D.S.Y., Chan, R., Brown, G., Ying, L., Sutejo, R., Aitken, J., Tan, B.H., Wenk, M.R., and Sugrue, R.J. (2009). Evidence that selective changes in the lipid composition of raft-membranes occur during respiratory syncytial virus infection. Virology *386*, 168–182. https://doi.org/10.1016/j.virol.2008.12.017.

36. Dai, P., Tang, Z., Qi, M., Liu, D., Bajinka, O., and Tan, Y. (2022). Dispersion and utilization of lipid droplets mediates respiratory syncytial virus-induced airway hyperresponsiveness. Pediatr. Allergy Immunol. *33*, e13651. https://doi.org/10.1111/pai.13651.

37. Heaton, N.S., and Randall, G. (2011). Multifaceted roles for lipids in viral infection. Trends Microbiol. *19*, 368–375. https://doi.org/10.1016/j.tim.2011.03.007.

38. Fedson, D.S., Opal, S.M., and Rordam, O.M. (2020). Hiding in plain sight: an approach to treating patients with severe COVID-19 infection. mBio *11*, e003988-20. https://doi.org/10.1128/mBio.00398-20.

39. Diseases, N.C.M.R.C.f.R. (2020). Chinese experts' consensus statement on diagnosis, treatment and prevention of respiratory syncytial virus infection in children. Chinese J. Appl. Clin. Pediatr. *35*, 241–250.

STAR★METHODS

KEY RESOURCES TABLE

REAGENT or RESOURCE	SOURCE	IDENTIFIER
Biological samples		
Serum	Children's Hospital Affiliated Capital Institute of Pediatrics	N/A
Critical commercial assays		
Pierce™ Top 12 Abundant Protein Depletion Spin Columns	Thermo Scientific	Cat#85165
Deposited data		
proteomics data	ProteomeXchange	PXD040110
Software and algorithms		
Perseus 1.6.15.0; R 3.6	max planck institute of biochemistry	https://www.maxquant.org/perseus/
MaxQuant_2.1.0.0	max planck institute of biochemistry	https://www.maxquant.org/
MSDIAL_3.70	RIKEN Center for Sustainable Resource Science	http://prime.psc.riken.jp/compms/msdial/main.html
MetaboAnalyst 5.0	metabolomics data analysis web	https://www.metaboanalyst.ca/
The Human Metabolome Database	small molecule metabolites database	https://hmdb.ca/
SPSS 13.0	Statistical Program for Social Sciences software	https://www.ibm.com/spss
Mfuzz v.2.46.0	Cluster software	https://www.bioconductor.org/packages/release/bioc/html/Mfuzz.html
Cytoscape v.3.2.1	National Institute of General Medical Sciences of the National Institutes of Health	https://cytoscape.org/
MeV v 4.7.4	Bio-informatics software	https://sourceforge.net/projects/mev-tm4/
Other		
uniprot-proteome_UP000005640_20220420.fasta	UniPro consortium	https://www.uniprot.org/(PXD040110)
C18 1.9 mm 150 μm × 120 mm	Thermo Scientific	25002-152130-V
C18 3 mm 100 μm × 20 mm	Thermo Scientific	22,103-052130

RESOURCE AVAILABILITY

Lead contact

Further information and requests for resources and reagents should be directed to and will be fulfilled by the lead contact, Jieqiong Li. jieqiongli2010@163.com.

Materials availability

This study did not generate new unique reagents.

Data and code availability

The proteome analysis datasets have been deposited at iProX and are publicly available as of the date of publication. Accession numbers are listed in the key resources table.

This paper does not report original code.

Any additional information required to reanalyze the data reported in this paper is available from the lead contact upon request.

EXPERIMENTAL MODEL AND SUBJECT DETAILS

Patient enrollment

RSVs and IDCs were recruited from the Capital Institute of Pediatrics from December 2021 to March 2022. Diagnosis of RSVs were made in accordance with the inclusion criteria: 1) symptoms, signs, and related auxiliary examinations which met the diagnostic requirements as described in the ''Chinese experts' consensus statement on diagnosis, treatment and prevention of RSV infection in children (2020 edition)'';[39] 2) RSV infections were verified by PCR; 3) younger than 18 years old. The exclusion criteria were: 1) specimen contamination; and 2) immunodeficiency. IDCs had symptoms including respiratory symptoms and was not RSV pneumonia. HCs were collected from children undergoing physical examinations at the Capital Institute of Pediatrics. This study was approved by the Capital Institute of Pediatrics ethics committee.

Clinical information

Complete clinical information, including C reactive protein (CRP), white blood cells (WBC), procalcitonin (PCT), and the proportion of blood cells [neutrophils% (Neu%), lymphocyte% (Lym%), monocytes% (Mon %)] were collected.

METHOD DETAILS

Metabolomic analysis

Serum samples from all RSV (n=64), IDC (n=46) and HC (n=52) enrolled in this study were collected for metabolomic analysis (Table S1). In each sample, 100 μL of patient sera was mixed with 400 μL of MeOH/ACN (1:1, v/v) and then incubated and centrifuged for 10 minutes at 13,500 × g at 4°C. The supernatant was then divided into two fractions: one for reverse-phase/ultra-performance liquid chromatography (RP/UPLC)-MS/MS methods and positive ion-mode electrospray ionization (ESI) and one for negative-ion mode ESI.[6,7] Quality control (QC) samples were obtained from all participants (equal amounts of 5μL), pooled and then divided into 6 samples. These samples were used to monitor the stability between runs. The MS-DIAL software and Human Metabolome Database (HMDB, https://hmdb.ca) were used to identify metabolites.

Proteomic analysis

A total of 44 samples (15 RSVs, 14 IDCs, and 15 HCs) were randomly collected from participants enrolled for proteomic analysis (Data S1). Briefly, tris phosphine (Pierce, USA) was added to the sera from each participant to reduce sulfide bonds. Next, iodoacetamide (Sigma-Aldrich, USA) was added to the mix for alkylation and incubated at 25°C in the dark with agitation at 300 RPM for 1 hour. The proteins were then digested with mass spectrometry-grade trypsin gold (Promega, USA) overnight at 37°C. Afterwards, 20μL of loading buffer (1% formic acid, FA; 1% acetonitrile, ACN) was used to dissolve the dried peptides and 10 μL of peptide was used for liquid chromatography-tandem mass spectrometry (LC-MS/MS) analysis. Peptides were quantified by peak areas obtained from MS1 intensities, and the protein intensities were calculated from the intensities of unique and razor peptides.[6,7]

QUANTIFICATION AND STATISTICAL ANALYSIS

Statistical analysis of clinical data

Statistical analysis was performed using SPSS 13.0. The differences between 2 groups were calculated using student's t-test while a one-way ANOVA was used to compare differences between HC, RSV, and IDC groups. P values < 0.05 was considered as statistically significant.

Statistical analysis of multi-omics data

For metabolomics, we set quality control (QC) for normalization, and pooled QC samples were prepared by mixing equal amounts of plasma from all samples. The pretreatment of the QC samples was performed in parallel and was the same as the other samples. The QC samples were evenly inserted between each set of runs to monitor the stability of the large-scale analysis. For proteomics, MaxQuant v2.1.0.0 was used for protein identifitcation and label free quantification (LFQ), correcting the original intensity between samples to eliminate inter-sample error caused by processing, sampling, pre-testing and the instrument. For each group compared, the fold-change (FC) and significance was calculated using the mean of each group and a two-sided unpaired Welch's t test. The selection criteria for differentially expressed proteins (DEPs) and

differentially expressed metabolites (DEMs) were set as follows: FC > 1.5 or FC < 0.67 with P value < 0.05. Partial least squares-discriminate analysis (PLS-DA) was conducted using MetaboAnalyst 5.0 and validated by a 10-fold method with unit variance scaling.

The intensity data of these regions were used for GraphPad analysis. Heatmaps were created using the Multi Experiment Viewer software (MeV, version 4.7.4). The Gene Ontology (GO) database was used to analyse GO biological processes (BP) Signaling pathway analysis was performed using the Kyoto Encyclopedia of Genes and Genome (KEGG) database and Metaboanalyst 5.0. Clustering models of proteins and metabolites were performed by Mfuzz v.2.46.0. Connected networks of the DEPs were performed using String, a plug-in for Cytoscape (v.3.2.1).

For biomarker selection and verification, a receiver operating characteristic (ROC) analysis was performed and the predictive power of each metabolite was ranked according to the ROC area under curve (AUC) value.